# 1 Introduction: Neurons, synapses, and the tiniest circuits

Our focus is on the dynamics and function of neuronal circuits. Dynamics is a common term in physics and describes how the state variable of a system evolves over time. Think of a hoop that rolls down an incline plane and just keeps on going, something you probably first learned about in a high school physics class. At the end of the day, you write equations for the linear (v) and angular (ω) velocity and, if the hoop rolls without slipping, then v $\propto \omega$ and life is particularly simple. One NEVER asks "What is the function of the hoop?". But biologists always ask about function. Here the loop may be part of a cart and the function of the hoop is to allow the cart to roll. Add a motor and the function of the loop is to transport the cart. Then one can ask "What is the function of the cart?" This line of questioning is never ending.

In neuroscience, the function of the nervous system is to compute something. In general, and somewhat like modern approached to robotics, there is a control layer and a cognitive layer. A control layer is close to the sensory input and motor output, like the preBötzinger circuit that controls breathing. Interestingly, this circuit was discovered by Jack Feldman, a physicist turned neuroscientist that chose the name Bötzinger after a bottle of northern German wine. The preBötzinger circuit is a group of a thousand neurons that sits at the base of the brain, i.e., near the ventral edge of the medulla (Figure 1). The computations involves an oscillator to set a rhythmic output and feedback from blood oxygen and body movement to modulate the rate of breathing. This is what a lot of circuits do - they control a motor output.

Figure 1: Axons from the preBötzinger complex that project to the parahypoglossal nucleus and the nucleus of the solitary tract regions (top) and ventral respiratory group complex (bottom). From Tan, Pagliardini, Yang, Janczewski and Feldman 2010.
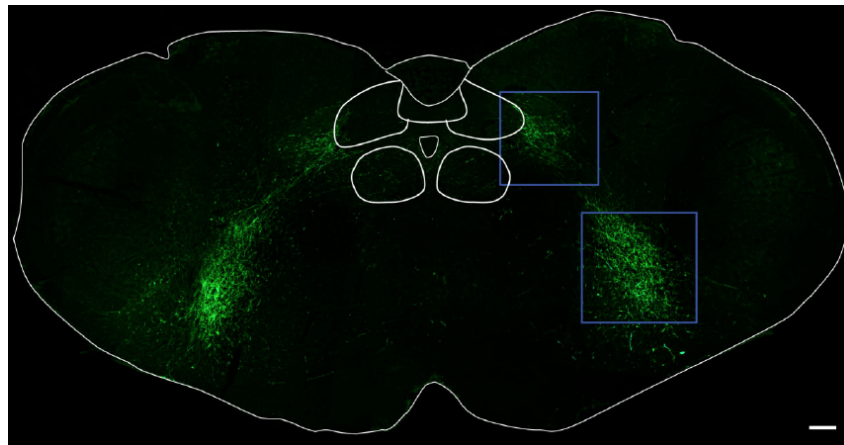
At the other extreme, is the cognitive function of a brain, This is the deep and so far dark secret of the brain which sets the course of future behaviors and, frankly, uses a calculus that we all would like to understand. For now, we will leave this to the psychologists. But we can us a tool like blood oxygen level dependent (BOLD) functional magnetic resonant imaging (fMRI), invented by Seiji Ogawa, to see where the brain activity is likely to be localized during different tasks (Figure 2). This is both crude and exciting at the same time, as we don't know what leads to abstract thought and problem solving, just that much of the brain appears to be involved in every task.

Figure 2: BOLD fMRI image of the human brain highlights increased metabolism during different mental activity. From Fox and Raichle 2007
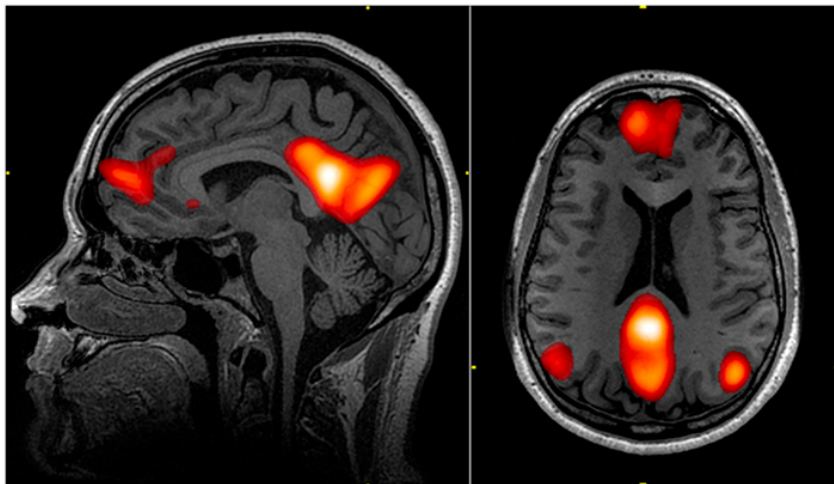
1.1 The shape of neurons

Neurons send out processes that gather inputs from a few to ten thousand inputs; these are called dendrites and normally extend over a spatial distance of 100 μm to 1 mm in mammals (Figure 3). In special cases like that of somatosensory cells, the distance that they have to communicate, such as from the tip of the toes to the spinal cord, is so long that they actively propagate their signal. Neurons integrate their many inputs from their dendrites within or near their soma. If the sum of all inputs exceeds a threshold, they produce an output spike (more on this later) that propagates down a long process, or processes, called axons (Figure 3). These can be up to meters in length. While cartoons of neurons draw them as rather stout, real neurons are spindly creatures. This is illustrated for three pyramidal cells from a massive reconstruction of 75,000 neurons, obtained from 30 nm resolution electron microscopy data. in the visual cortex of a mouse (Figure 4). Some neurons have processes that can span the entire brain with a labyrinth of axons, as seen in a light–level reconstruction of a secondary sensory cell, whose body, or soma, is in the trigeminal nucleus but whose axons sprout broadly to multiple targets (Figure 5).

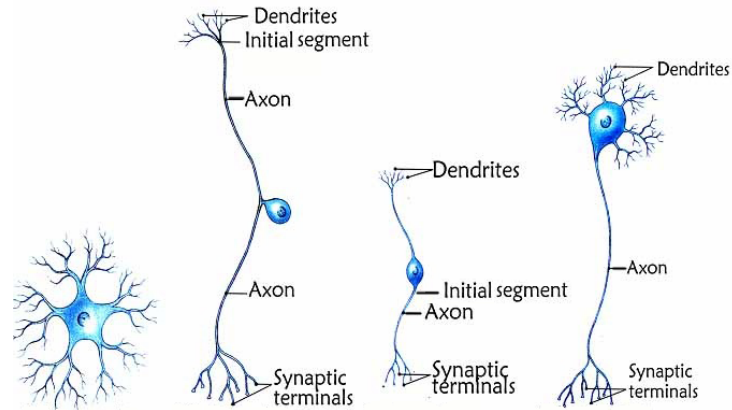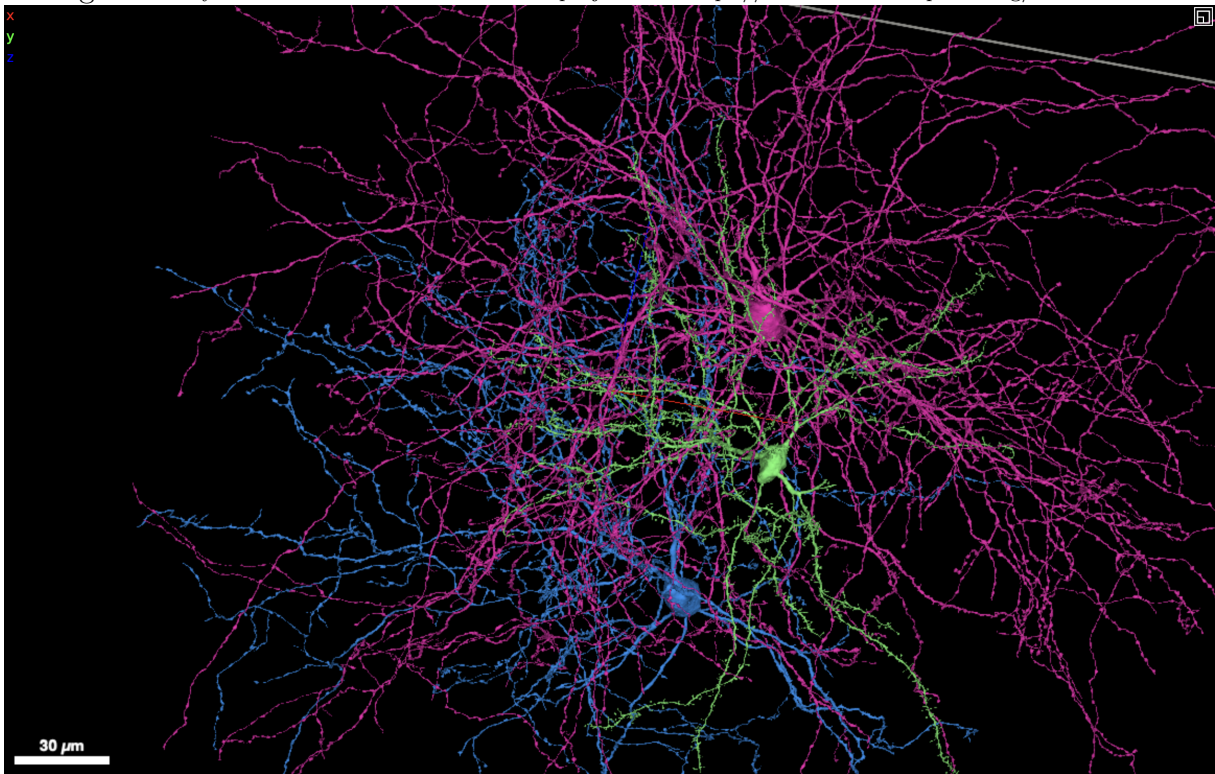Figure 3: The classic cartoon of different types of neurons. Source unknown.

Figure 4: Pyramidal neurons from the Microns project. See https://www.microns-explorer.org/cortical-mm3.

1.2 Neurons signal with pulses

Neurons signal with spikes, so called action potentials, as first shown by Kenneth Cole in 1939. These signals look like derivatives in time of a rising edge (Figure 6).

We now step back and visit the nature of spike generation by neurons (Figure 7). We'll do this first in terms of an ad hoc simplified model, and return to a detailed description later.

Figure 5: A neuron from the spinal trigeminal nucleus interpolaris and its targets. This spiking output of this cell codes the valence of a stimulus. Elbaz, Callado-Perez, Demers, Kleinfeld and Deschenes, 2022.
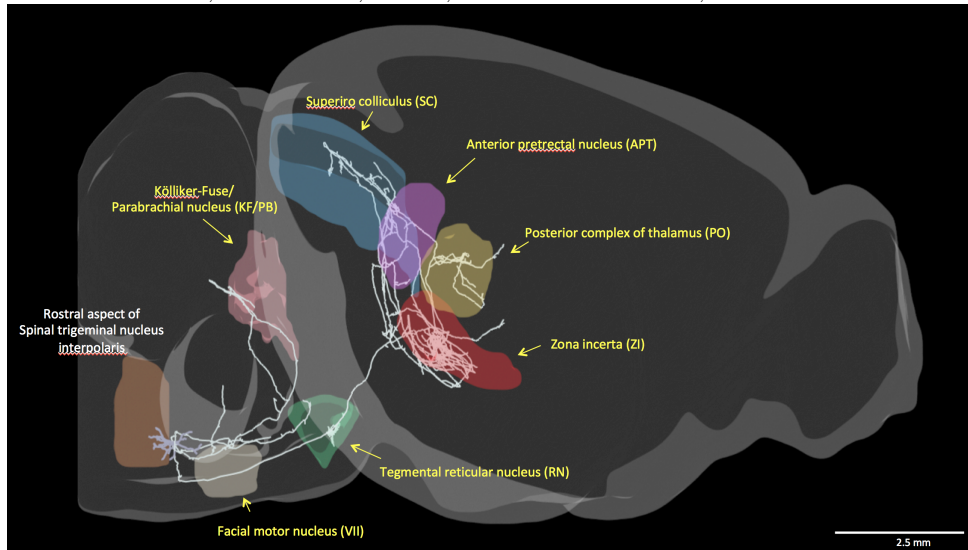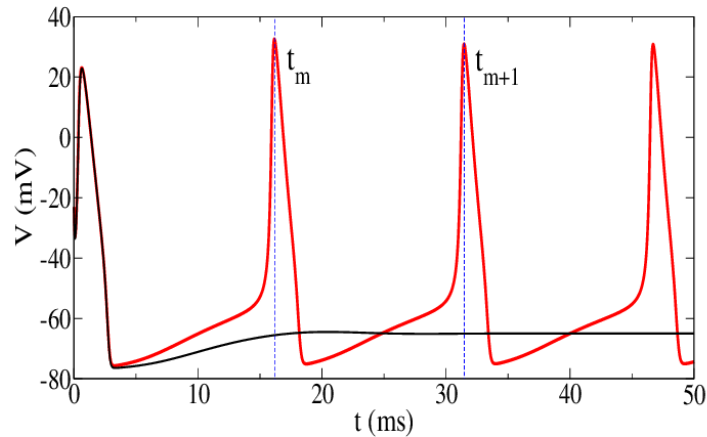

Figure 6: Calculated Hodgkin Huxley neuronal action potential in response to a pulse (black) and in response to a constant input (red). Source unknown.


1.3 Fundamental nonlinearity for an action potential

Neurons have a few essential components (Figure 8):

- An inside and an outside with a wall, the cell membrane, that hold ion pumps and ions channels in place.

- A sodium/potassium exchange pump that makes the inside high in potassium and low in sodium.

- Ion selective channels for the movement of sodium and and for potassium. This sets

4

Figure 7: Spikes are the currency of neuronal computation and communication. From Bellavance, Takatoh, Lu, Demers, Kleinfeld, Wang and Deschenes, 2017.
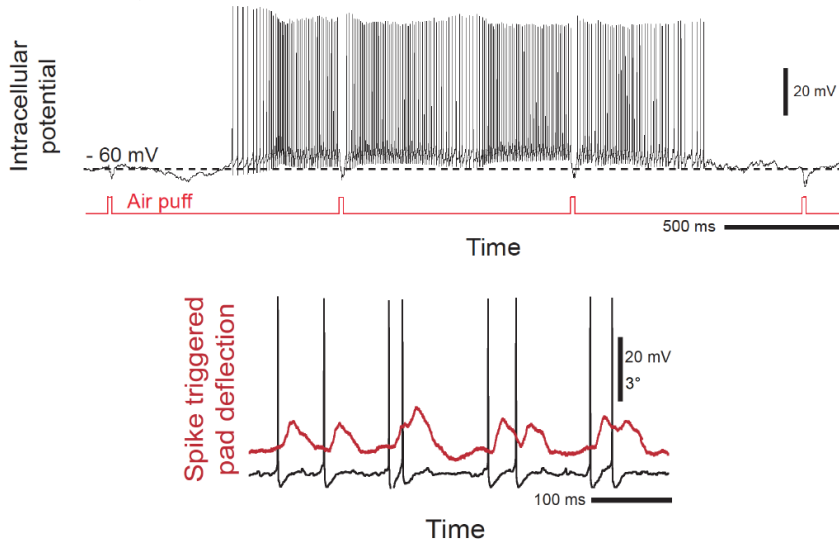
up two potentials, a high potential

$$V_{Na^+}^{\text{Nernst}} = \frac{k_B T}{e} \log_e \frac{[Na^+]_{outside}}{[Na^+]_{inside}} \tag{1.1}$$

where $\frac{k_B T}{e} \approx 25$ mV is the thermal voltage scale and the the sodium reversal potential is $V_{Na^+}^{\text{Nernst}} \approx +70$ mV, and a low potential with

$$V_{K^+}^{\text{Nernst}} = \frac{k_B T}{e} \log_e \frac{[K^+]_{outside}}{[K^+]_{inside}} \tag{1.2}$$

where the potassium reversal potential is $V_{K^+}^{\text{Nernst}} \approx$ -85 mV,

- Ion selective channels that further have their conductance gated by the membrane voltage. We focus on the voltage sensitive ion channel for Na^+. This is an essential ingredient that allows signaling. The threshold for switching the ion conductance from a nonconducting to a maximally conducting state is θ with $\theta \approx$ -45 mV.

We see that the neuron can integrate inputs in the range between $V_{K^+}^{\text{Nernst}}$ and V_{thresh} .

Let us consider a minimal circuit that shows haw a single voltage-dependent conductance leads to an instability and the the threshold phenomena in neuronal spiking (Figure 10) For small disturbances of the membrane potential, the cell returns to the resting potential. However, for current injections beyond some critical value, the potential will jump to a new equilibrium point. A simplified model makes use of a voltage dependent change in the conductance for one of two ions. To be concrete, we take a cell with a solely Ohmic potassium current, G_{K^+}, and a voltage dependent sodium conductance, $G_{Na^+}(V)$, that has a value of zero below a threshold potential, V_{th}, and that is constant above V_{th} with value $G_{Na^+}(V_\infty)$.

Figure 8: The voltage scales for a neuron. Most of the time the cell is in the ranges defined by the thick black bands for integrating or communicating.
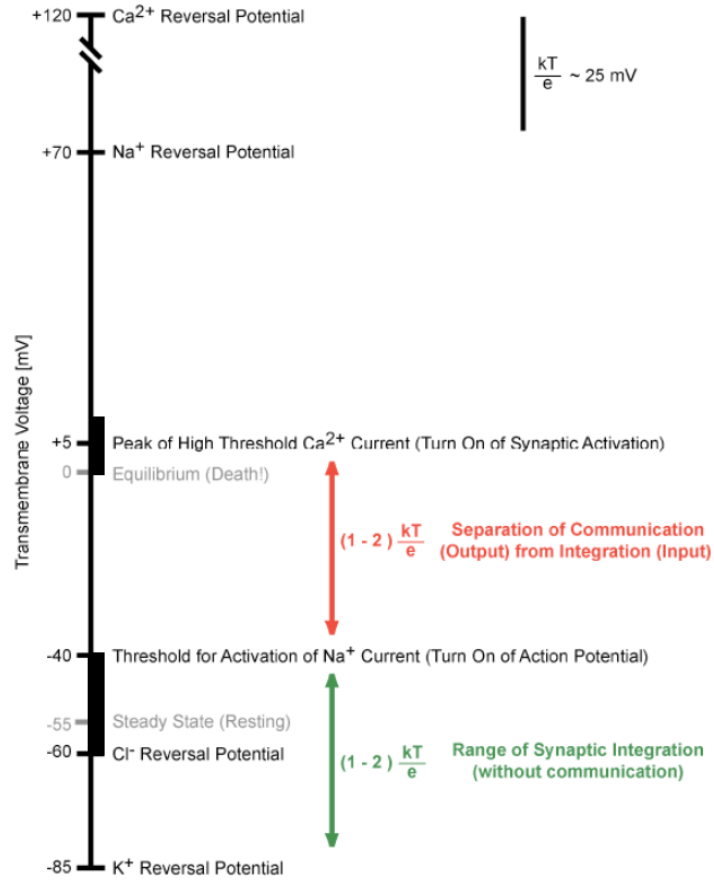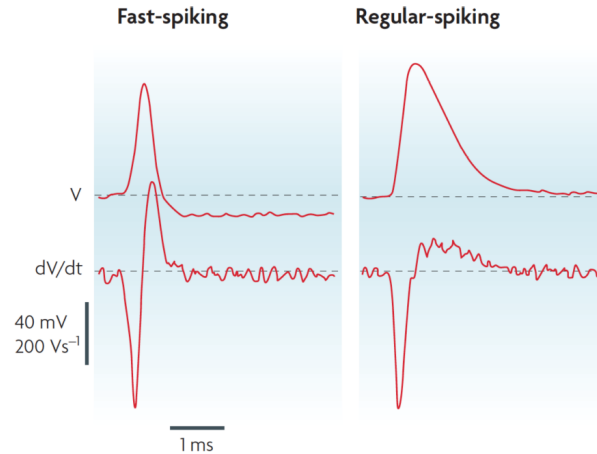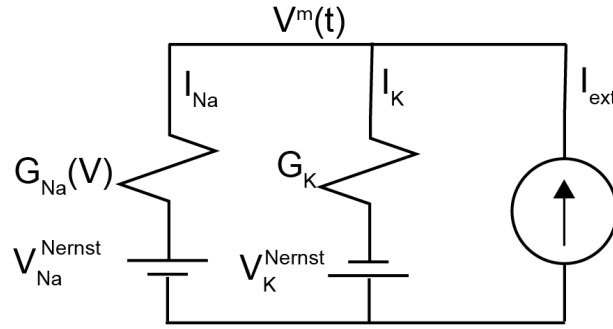

Figure 9: The Na^+ current leads to a similar rise across different classes of neurons. From McCormick, Connors, Lighthall and Prince, 2009.

Thus we have a current-voltage relation given by

$$I(V) = \begin{cases} G_{K^+}(V - V_{K^+}) & \text{if } V < \theta \\ G_{K^+}(V - V_{K^+}) + G_{Na^+}(V_\infty)(V - V_{Na^+}) & \text{if } V > \theta \end{cases} \qquad (1.3)$$

Figure 10: The circuit for two conductances, one fixed and the other that turns on above V_{thresh}.

where, V_{Na^+} and V_{K^+} are the Na^+ and K^+ Nernst potential for sodium and potassium, respectfully' we'll return to this. This relation is discontinuous at $V = \theta$ and Ohmic below and above this potential (Figure 11). There are two equilibrium values, one for $V < \theta$ and one for $V > \theta$. These are found by setting $I(V) = 0$, so

$$V_{equil} = \begin{cases} V_{K^+} & \text{if } V < \theta \\ \frac{G_{K^+}V_{K^+}+G_{Na^+}(V_\infty)}{G_{K^+}+G_{Na^+}(V_\infty)} & \text{if } V > \theta \end{cases} \tag{1.4}$$

Figure 11: The onset phase of an action potential. The data (left) shows the onset occurs just above a threshold current of $I = 1.00$ (source unknown), while the cartoon shows how a change in the total conductance at threshold voltage, θ, leads to a bistable behavior and switching of the stable point from rest to top of the action potential.
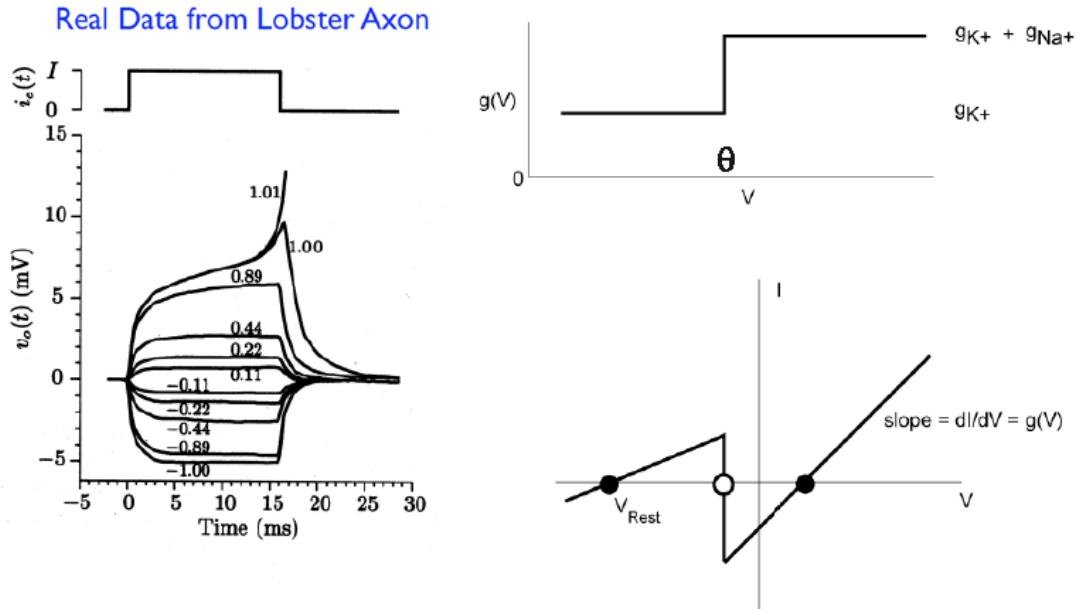
We consider a pulse of current that causes the cell to change from the lower to the upper curve. This represents the front of the action potential. The shift in equilibrium potential from V_{K^+} to $\frac{G_{K^+}V_{K^+}+G_{Na^+}(V_\infty)}{G_{K^+}+G_{Na^+}(V_\infty)}$ occurs in roughly $10^{-4}s$ (Figure 11). On the

7

longer time scale of $10^{-3}s$, relaxation processes associated with the Na^+ current and the activation of an additional voltage dependent K^+ current cause the front to decay. Thus the nonlinearity in Figure 11 decays into a monotonic relation and the neuron recovers (Figure 12).

Figure 12: The slower recovery phase of an action potential. The Na^+-current begins to turn-off and a K^+ current turns on and the membrane potential returns to rest.
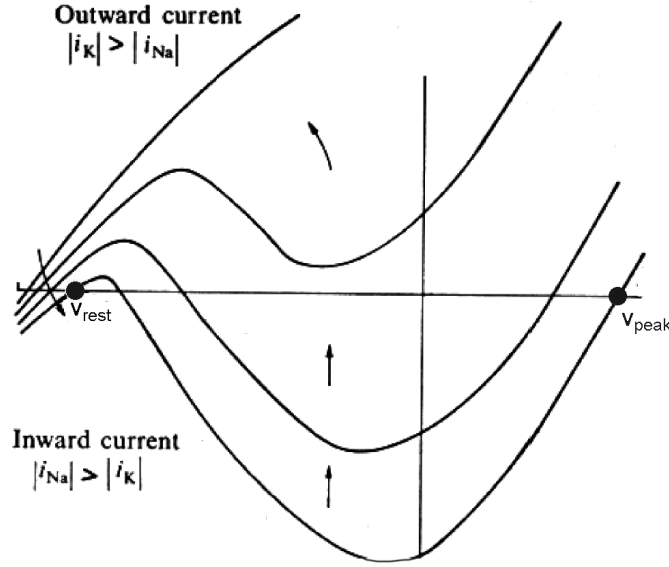

We are left with a pulse (Figure 6). The key issue is that neurons use two voltage levels, and at least one voltage dependent conductance, to shift between the two levels.

Figure 13: Estimation of the firing rate of a neuron and the complete input-output curve. Source unknown.
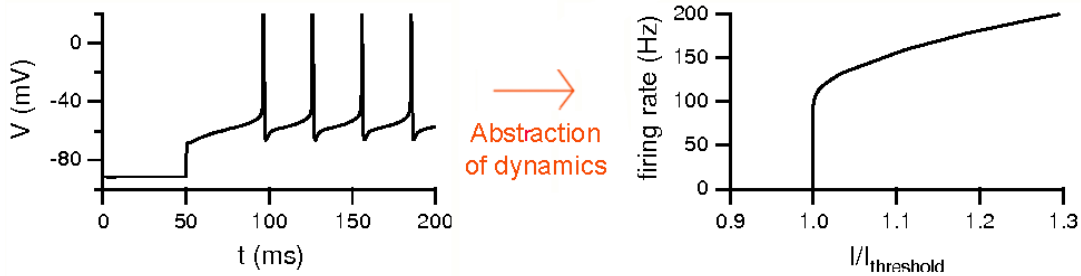
Suffice it to say that neurons are quiet until the input exceed a threshold level, and then they spike with a spike rate that is monotonic with the input current (Figure 13). The description in terms of a rate, which abstracts away the details of voltage changes during spiking in favor of slowly varying rate, is one that we adopt. While the rate for Hodgkin-Huxley neurons shows a jump in the shape of the rate-input curve at threshold (Hopf bifurcation), neurons with a plethora of channels can have dynamics that lead to a smooth increase in rate above threshold (saddle node bifurcation) (Figure 14).

Figure 14: Calculated spike rate for a motoneuron in the facial nucleus in response to different input currents and adaptation currents. Golomb, Moore, Fassihi, Takatoh, Prevosto, Wang and Kleinfeld, 2022
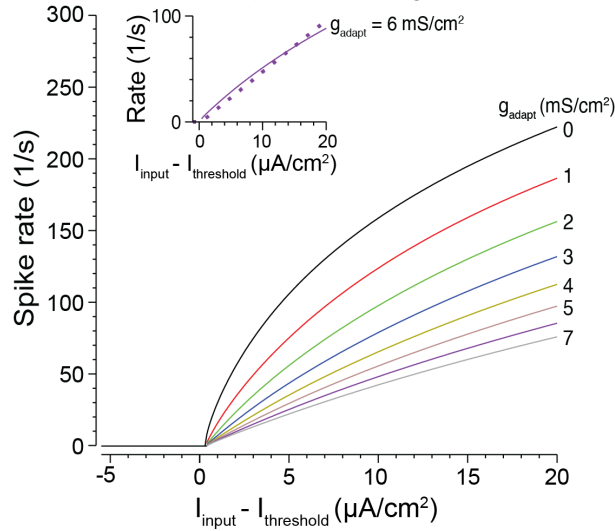
1.4 Communication is unidirectional

Electrical isolation of one neuron from another is achieved by a communication mechanism that converts an electrical signal to a chemical cascade (Figure 18), and then converts that back to an electrical signal. Thus communication is unidirectional and the sign and strength of the communication depends on both pre- and post-synaptic elements.

Neurons signal through structures called synapses, which convert the voltage of an action potential in the presynaptic neuron (V_{soma} in Figure 18) into either a depolarizing or hyperpolarizing current in the postsynaptic neuron (Figure 17). They do this in a circuitous path, with the pulses in voltage in the presynaptic cell (V_{pre} in Figure 16) cause an ion, Ca^{2+}, to flow into the presynaptic bouton (I_{Ca} in Figure 16) . This process is dominated by activation of a high-threshold voltage gated Ca^{2+} current, whose current peaks at around 0 mV or near the peak of the action potential. A typical example id the CaV2.2 channel.(Figure 15). The key feature is that the Ca^{2+} is negligible below the threshold for a spike.Further, this influx of Ca^{2+} can lead to a further increase through Ca^{2+}-induced Ca^{2+}-release from the endoplasmic reticulum.

The high influx of Ca^{2+} ions cause vesicles with neurotransmitter molecules to fuse with the membrane and release their molecules across a narrow cleft ($P_{release}$ in Figure 16) . These bind to neurontransmitter receptor channels in the postsynaptic spine and induce a postsynaptic current ($EPSC$ in Figure 16) and concurrent postsynaptic voltage (V_{post} in Figure 16). The entire process consumes about 1 ms of delay time.

Many molecular steps are involved in the fusion process of vesicles to release neurotransmitter molecules into the synaptic cleft (Figure 18), a space of 10 nm in width and 1 μm is lateral extent (Figure 17).

The neurotransmitter molecules bind to protein channels in the postsynaptic cells that transiently open and allow ions to rush through. Thus a voltage on the presynaptic side of the synapse is converted to a current on the postsynaptic side. This current

Figure 15: CaV channel nomenclature and properties. Left. Voltage-gated Ca^{2+} channel homology, human genetic nomenclature, and protein classification. The channels are divided into three main groups, CaV1, CaV2, and CaV3, on the basis of homology and are then subdivided according to the individual gene products. The tissue distribution and main functions of each isoform are listed. RIght. Normalized current-voltage relationships for CaV currents recorded from cultured cells. A comparison of the activation voltage ranges of CaV3.1, CaV1.3, CaV1.2, and CaV2.2 channels shows that there is a continuum of activation voltages for the different channels. From Dolfin and Lee, 2020.
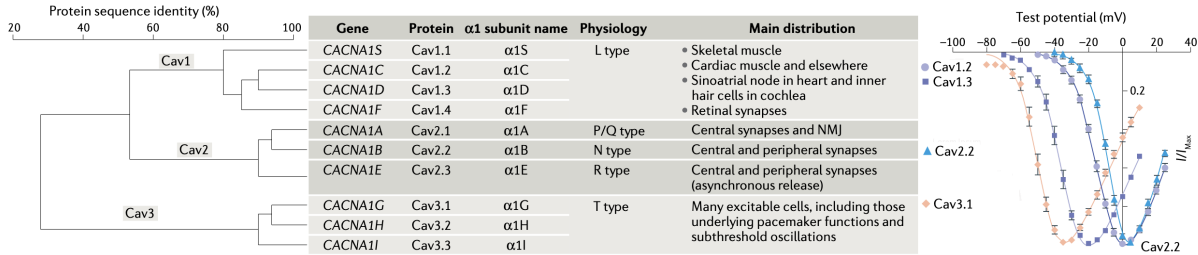

Figure 16: Events in synaptic transmission. An action potential is fired at the cell body (V_{soma}) and propagates into the presynaptic terminals (V_{pre}) and generates a calcium current (I_{Ca}) near the neurotransmitter release site to increase the probability of vesicle fusion ($P_{release}$). Released neurotransmitter generates an excitatory postsynaptic current (EPSC) that depolarizes the postsynaptic cell (V_{post}) and causes it to fire an action potential. From Sabatini and Regehr, 1999.
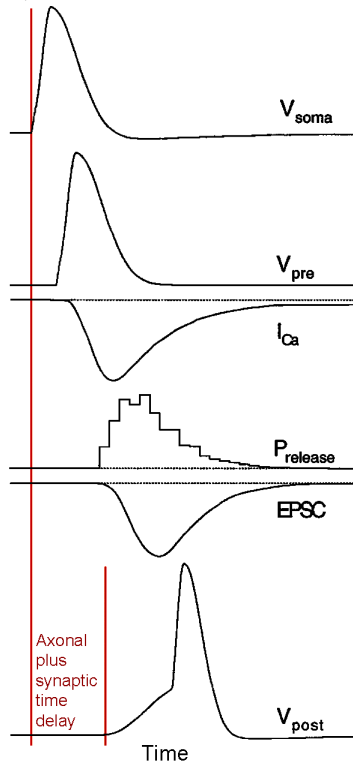
is observed as a change in post-synaptic voltage The signaling is solely one-way, from pre-synaptic to post-synaptic neurons. This is much like the functional operation of a field effect transistor, although the physics is completely different. Measurements of synaptic transmission show that each synaptic events leads to a change of potential in the postsynaptic cell that appears bimodal, with one peak at around 1.5 mV, that likely

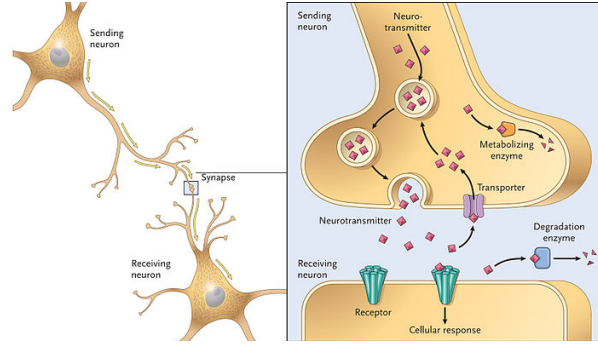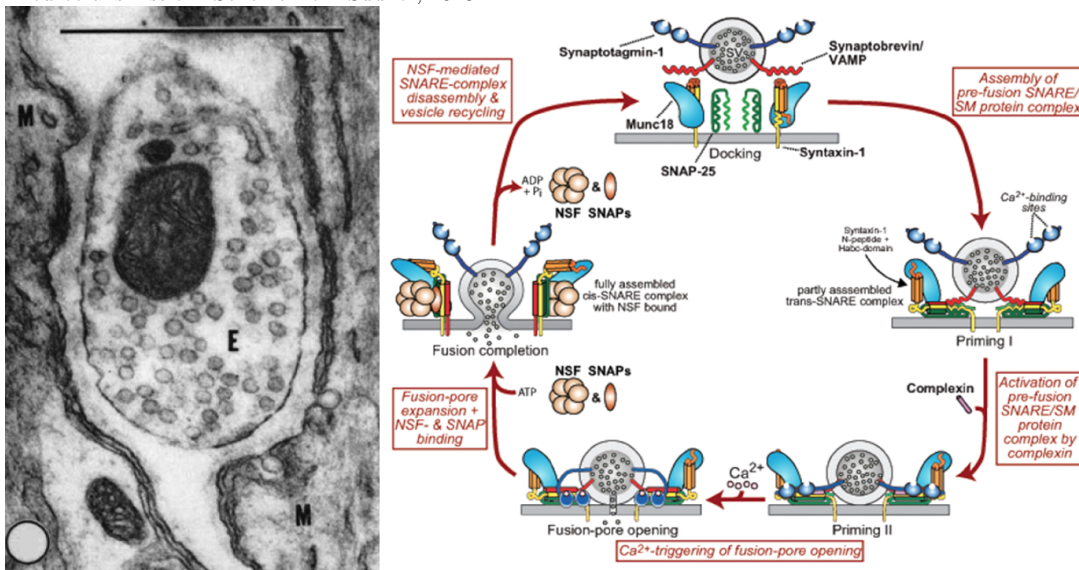Figure 17: Cartoon of synaptic function. Source unknown.

Figure 18: Electron micrograph of a synapse and scheme of the SNARE/SM protein fusion scheme that regulates Ca^{2+} driven neurotransmission. Scheme from Sudhof, 2013

reflects multiple contacts between the same pairs of cells, to a peak near 0.5 mV after all but one synapse is depressed (Figure 19). Even for the large value, this means that input from one presynaptic cells is insufficient to activate a post-synaptic cell and that roughly ten synchronous presynaptic inputs are required, or 100 asynchronous inputs. This sounds like a lot - but as we saw neurons typically have 10,000 inputs. The key issues for computation are

- Directionality: Complicated molecular process of synaptic transmission ensures that signaling is unidirectional.

- Isolation: Dendritic integration *per se* cannot lead to synaptic release, nor communication, until the threshold for spiking is crossed.

We summarize the impact of a synapse by a single number, the weight W. More specifically, we define $W_{i,j}$ as the synaptic weight from presynaptic neuron j to postsynaptic neuron i.

11

Figure 19: Pair-wise recordings from two synaptically connected cat layer 6 pyramidal cells. The presynaptic pyramid (orange soma/dendrites, white axon) resembles a claustrally projecting cell with a slender apical dendrite reaching layer 3 and an axonal arbor confined to the deep layers. The postsynaptic pyramid is a cortical-thalamic-like pyramidal cell (soma/dendrites yellow, axon grey) with an apical dendritic tuft and extensive axonal arborization in layer 4. (A) The EPSP resulting from this connection exhibited paired pulse and brief train depression that were more pronounced and involved a larger proportion of apparent failures of transmission (B) at shorter interspike intervals. From Mercer, West, Morris, Kirchhecker, Kerkhoff and Thomson, 2005
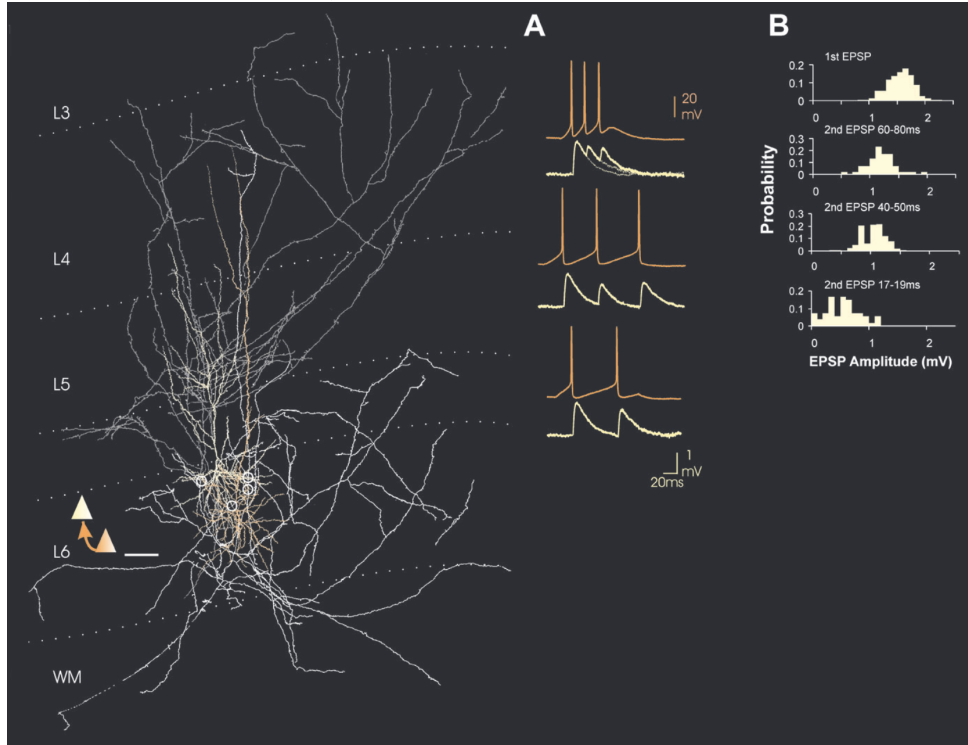
1.5 The simplest circuit - one neuron and one synapse

The simplest function is memory. We wish to remember the presence of a signal until we reset the network. As such, we consider the use of positive feedback to build a memory circuit. Let's consider the evidence and we will make a model. We can use a single synapse for form such positive feedback. This circuit exist in the mollusc Aplysia (Figure 20). Impressively, a buccal ganglion motor shows that an excitatory input from cell B63 to cell B31 and B32 leads to remembrance of the pulse (Figure 21A) and sustained muscular output to drive feeding in this mollusc. Inhibition, i.e., a hyperpolarizing input to cell B31 or B32 rests the output of the cell. (Figure 21A). A number of controls point to feedback (Figure 21B). These include the blocking of the sodium channels and the blocking of synaptic transmission.

We can understand this circuit in terms of a model with feedback (Figure 22A), i.e., one neuron and one synapse. A linear equation to describe subthreshold behavior is

$$\tau \frac{dV}{dt} + V = I^{ext} + I^{autapse} \tag{1.5}$$
$$= I^{ext} + WV$$

where $I^{autapse}$ is the feedback current through an autapse, i,e,, a synapse that a neuron

12

Figure 20: The relevant anatomy of a buccal circuit for sustained feeding. From Miller, Hurwitz and Susswein, 2009.
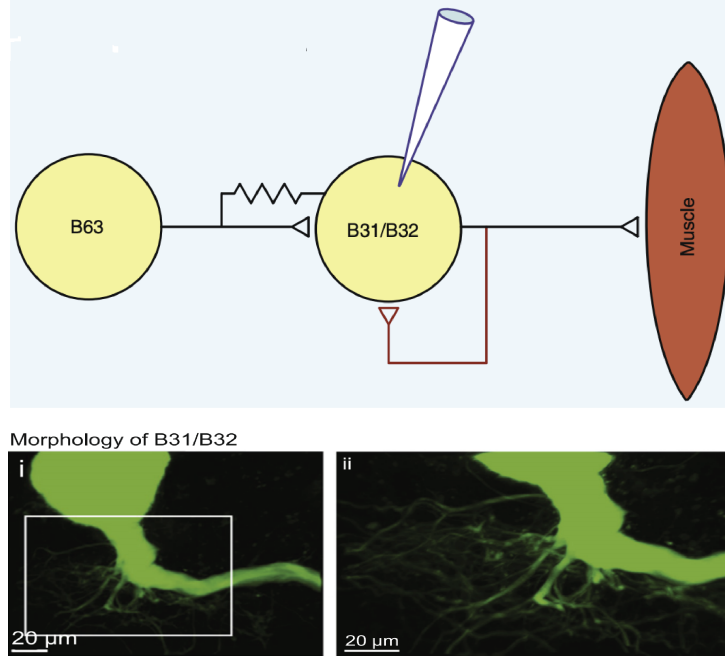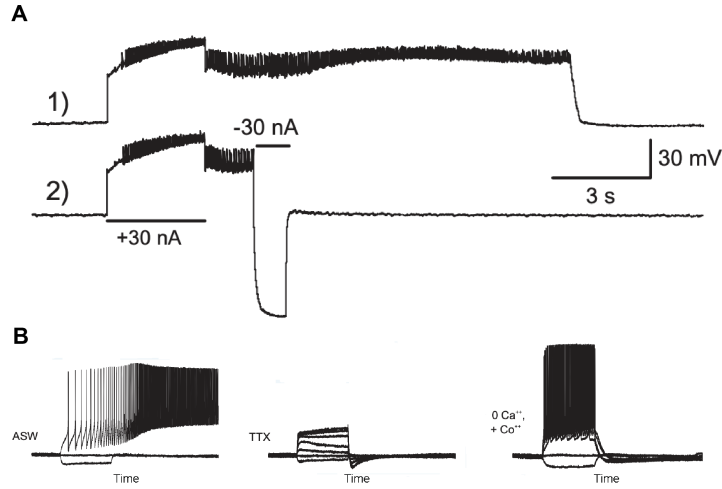

Figure 21: Recording from buccal ganglion neuron. A. The essential result showing persistent activity. B. Control experiments that quench spiking (TTX) or quench synaptic transmission (0 [Ca^{2+}]. From Saada, Miller, Hurwitz and Susswein, 2009.


makes onto itself, that we take as linear in V. Thus

$$\tau \frac{dV}{dt} = (W - 1)V + I^{ext} \tag{1.6}$$

which leads to stable (W < 1), meta-stable or memory (W = 1), and unstable (W > 1) behavior (Figure 22B). So we are on the right track.

To prevent run away instability for W > 1, we add a saturating inout-output relation $S(V)$ (Figure 23), where $S(V)$ can be considered as the firing rate . This leads to an output that saturates in one of two states, which we take as $S(V) = 1$ for maximal firing

Figure 22: A. Circuit. B. Behavior for different feedback strengths W. From MIT9-40S18-Lec20 (2018).
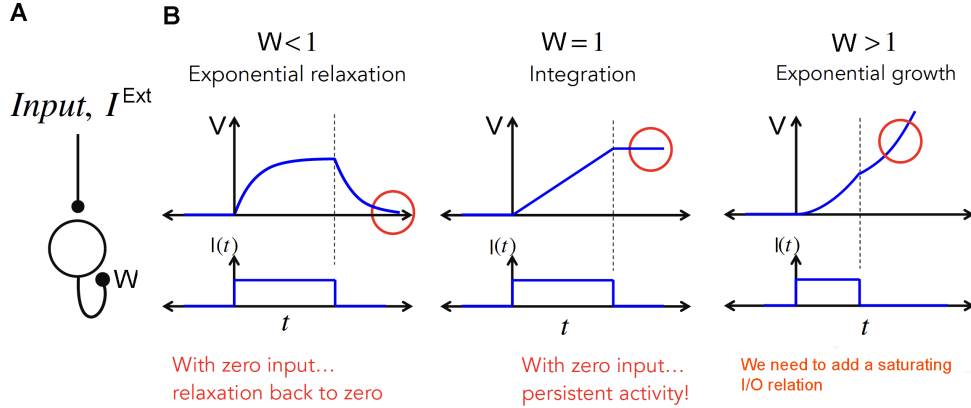
and $S(V) = -1$ for quiescence. The simplest choice is

$$S(V) = tanh(V) \tag{1.7}$$

which is linear for small values of V, i,e., $S(V) \to V$ for $V << 1$ and thus has a slope of $dS(V)/dV = 1$ at $V = 0$. Then

$$\tau \frac{dV}{dt} + V = I^{ext} + WS(V) \tag{1.8}$$

and at equilibrium

$$S(V) = \frac{V - I^{ext}}{W}, \tag{1.9}$$

which will always have two solutions for $I = 0$ since $W > 1$, is active with $S(V) \to +1$ for $I^{ext} >> 0$ and quiescent with $S(V) \to -1$ for $I^{ext} << 0$ (Figure 24).

We will next take this to the extreme and only consider dynamics in terms of neurons saturating outputs.

1.6 Threshold units can be used to build circuits

We can brutalize the input-output relation (Figure 23A) further and think in terms of binary quantities (Figure 25), so that the output is now "spiking" or "quiescent", much like the "0" and "1" signals in digital logic.

$$S_i \equiv sgn\left(\mu_i - \theta_i\right) \tag{1.10}$$

where μ_i is the input to the cell, from synapses and external drive, θ_i is the threshold, and we take the sign function to be

$$sgn(x) = \left\{ \begin{array}{rl} 1 & \text{if } x \geq 0 \\ -1 & \text{if } x < 0 \end{array} \right.$$

These threshold units can be used to build circuits for memory and computing . In fact, despite the complicated dynamics of biological neurons and the myriad of models

14

Figure 23: A. Saturating function. B. Effect of saturation to yield bistable output. From Fee MIT9-40S18-Lec20 (2018).
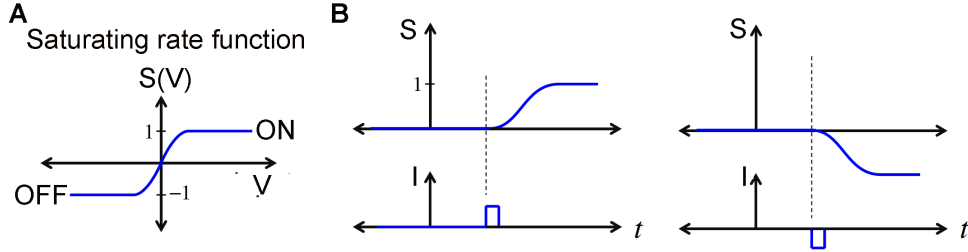

Figure 24: Bistable output with the addition of a saturating I/O function. From Fee MIT9-40S18-Lec20 (2018).
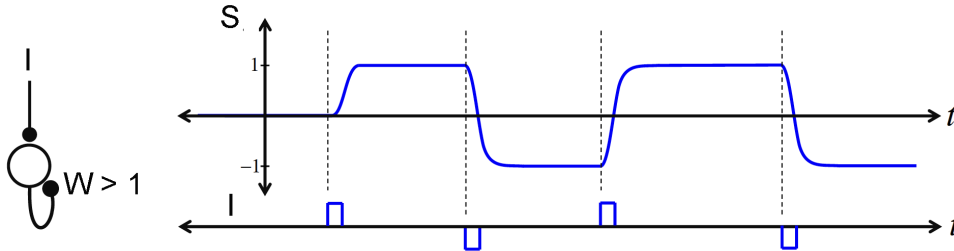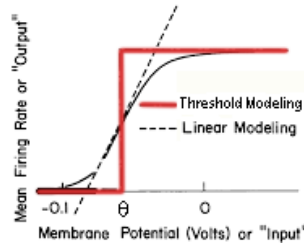

Figure 25: Model of a neuronal input-output in terms of a threshold function. Source unknown.

to capture these properties, we can get pretty far toward understanding computation in brains using just threshold units.

The simplest neuronal circuit has two neurons with output patterns labeled $\vec{\mathbf{S}}$, i.e.,

$$\vec{\mathbf{S}} = \left(\begin{array}{c} \text{output of neuron 1} \\ \text{output of neuron 2} \end{array} \right)$$

There are four possible output patterns, i.e.,

$$\vec{\mathbf{S}} = \left(\begin{array}{c} +1 \\ +1 \end{array} \right) \text{ or } \left(\begin{array}{c} -1 \\ +1 \end{array} \right) \text{ or } \left(\begin{array}{c} -1 \\ -1 \end{array} \right) \text{ or } \left(\begin{array}{c} +1 \\ -1 \end{array} \right)$$

1.7   Physical and biological flip-flops

It was known since the 1930's that bistable devices formed from threshold elements, like a digital flip-flop (Figure 26), could be built using feedback to hold electronic summing junctions in a particular state after their inputs had decayed away. Let's see how to use

15

two neurons to build a circuit that restricts the output to only two states, called stable states, denoted

$$\vec{\zeta_1} = \begin{pmatrix} +1 \\ -1 \end{pmatrix} \text{ and } \vec{\zeta_2} \begin{pmatrix} -1 \\ +1 \end{pmatrix}$$

Figure 26: The set-reset flip flop, with further gates at the input to turn it into a toggle or D flip flop. Black circles denote inhibition. Source unknown.
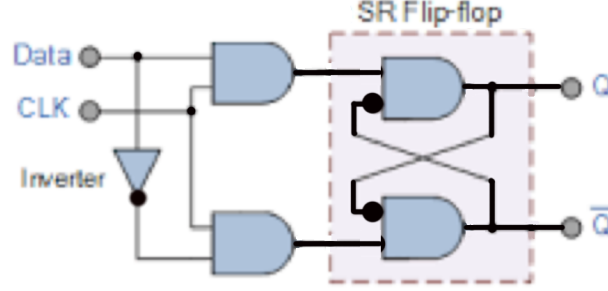
1.7.1 Neuronal flip-flops

We are motivated by electronics, where inhibitory feedback between two gates is used to make a flip-flop (Figure 26). Using our model for saturating output $S(V)$ (Figure 25), this circuit can be formed from two neurons and two synapses (Figure 27). The input of each neuron comes from two sources, external inputs denoted I_i^{ext} and inputs from other neurons through connections, i.e., synapses, with analog-valued synaptic weight W_{ij} . The total input to neuron i is:

$$
\begin{aligned}
\mu_i &\equiv \text{ input to neuron i} \\
&= \sum_{j=1;\, j\neq i}^{N} W_{ij}S_j + I_i^{ext}
\end{aligned}
\tag{1.11}
$$

where N is the number of neurons. Each neuron samples its input at random times. It changes the value of its output or leaves it fixed according to a threshold rule (Figure 25)with thresholds θ_i;.

$$
\begin{aligned}
S_i &\leftarrow -1 \text{ if } \sum_{j=1;\, j\neq i}^{N} W_{ij}S_j + I_i^{ext} < \theta_i \\
S_i &\leftarrow +1 \text{ if } \sum_{j=1;\, j\neq i}^{N} W_{ij}S_j + I_i^{ext} > \theta_i
\end{aligned}
\tag{1.12}
$$

If we take the case of two neurons, with $W_{12} = W_{21} = -1$ and for simplicity $I_1^{ext} = I_2^{ext} = 0$ and a threshold near zero, then we see that $\vec{\zeta_1}$ and $\vec{\zeta_2}$ are stable outputs. This circuit can be drawn in "Neural Network" style as nested feedback loops (Figure 28); this already suggests the extension of the feedback viewpoint to loops with very many cells.

Figure 27: Two model neurons and two inhibitory synapses, act as a flip-flop or bistable circuit that can be triggered to change state with a transient input. Black circles denote inhibition.
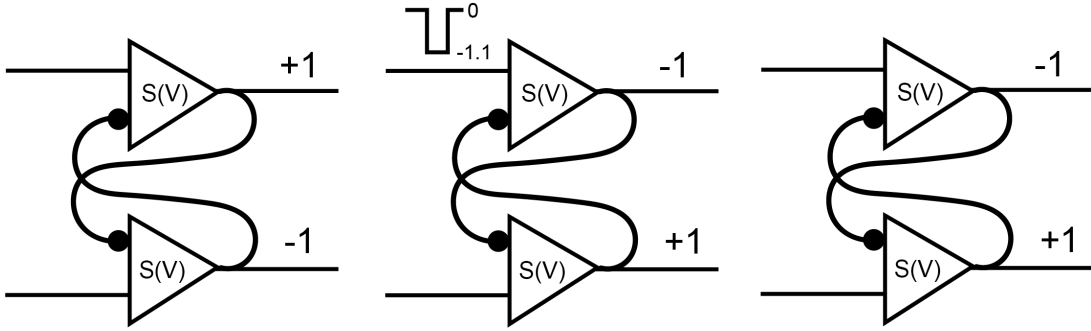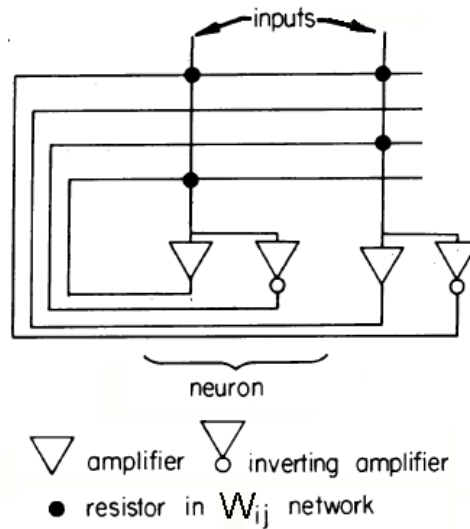

Figure 28: A two-neuron feedback circuit drawn in "Neural Network" style. Hertz, Krogh and Palmer 1991, following Hopfield 1982.

1.7.2 Setting the threshold

We want a cell to respond to its inputs, which means that the $\sum_j^N W_{ij}S_j$ terms must drive the neuron back and forth across the the threshold. In a sense, the inputs, their synaptic weights, and the value of the threshold are interconnected. To see this, we first denote the input to the cell, μ_i, as,

$$\mu_i \; = \; \sum_{j=1;\, j \neq i}^{N} W_{ij}S_j + I_i^{ext} \tag{1.13}$$

and the output as

$$S_i(\mu_i \; - \; \theta_i). \tag{1.14}$$

The best estimate for the value of θ is found from the average mid-point of the input to the cell. We thus average the input over time, denoted $< \cdots >$. Then

$$\theta \;\; = \;\; < \mu_i > \tag{1.15}$$

17

$$= \sum_{j \neq i}^{N} W_{ij} <S_j> + <I_i^{ext}>$$
$$= <I_i^{ext}>$$

where we assumed equal activity for all neurons, so $<S> = 0.5 * (-1 + 1) = 0$. Thus, for our choice of representation $S_i = \pm 1$ and no eternal input, the optimal threshold is $\theta = 0$.

1.7.3 Neurons that act as threshold units can be used to build biological circuits

We saw that biological neurons have input-output relations that appear as threshold phenomena. Can we use these to make model networks, in the dish, that illustrate this basic functions. This was accomplished back in ca 1990 using neurons dissected from the invertebrate Aplysia (Figure 29). Let check out the issues. First, we see that the neurons fire nearly as threshold units, albeit each cell has its own value of the threshold, θ. We also see that the neurons make inhibitory connections so that $\text{sign}[W_{12}] = \text{sign}[W_{21}] = $ -1. Then

$$\mu_1 - \theta_1 = -|W_{12}|S_2 - I_{O1}^{ext} - \theta_1 \qquad (1.16)$$
$$\mu_2 - \theta_2 = -|W_{21}|S_1 - I_{O2}^{ext} - \theta_2$$

Figure 29: A two-neuron circuit with reciprocal inhibition in vitro, and the F-I curves and synaptic response curves of the two cells. From Kleinfeld, Raccuia-Behling and Chiel 1990.
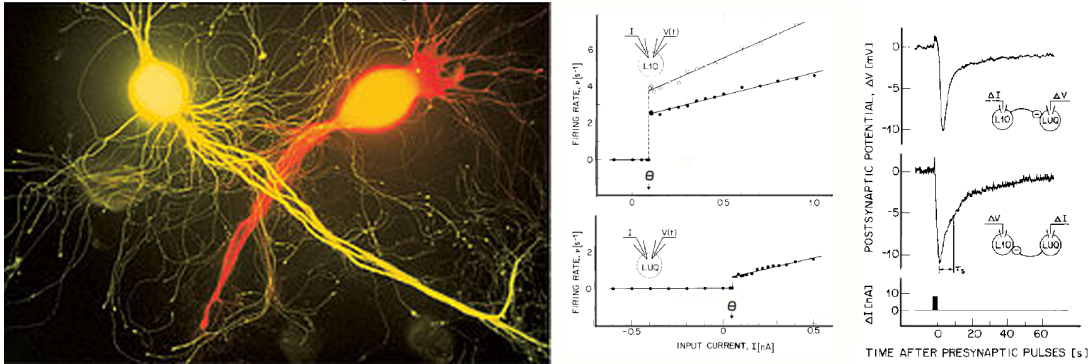
When combined together, we see that the circuit functions as a flip-flop with reciprocal inhibitory connections. A pulse into the "off" cell will drive it "on" and inhibit the neighboring cell, driving it "off" (Figure 30). The network is now stable in the new state. A key issue in considering only cells as "on" or "off", is that the synaptic integrations must be slow enough to average other individual spikes; this holds for the more general case of considering rates. In the case of the neuronal flip-flop as the spike rates are one to a few Hertz while in integration time is about 10 seconds.

The in vitro circuit allowed us to explore how the output can be pinned by large inputs, i.e., the effect of I^{ext} terms relative to the threshold θ (Figure 31). The data also illustrate that the magnitude of the synaptic input $|W_{1,2}S_2|$ must be large enough to change the sign of $I_1^{ext} - \theta_1$, and vice versa.

18

Figure 30: A two-neuron circuit in vitro with reciprocal synapses that shows bistability. From Kleinfeld, Raccuia-Behling and Chiel 1990.

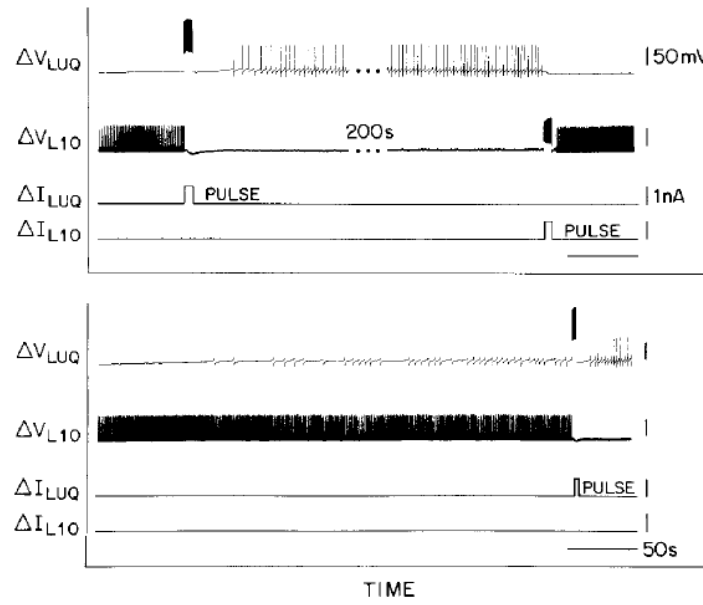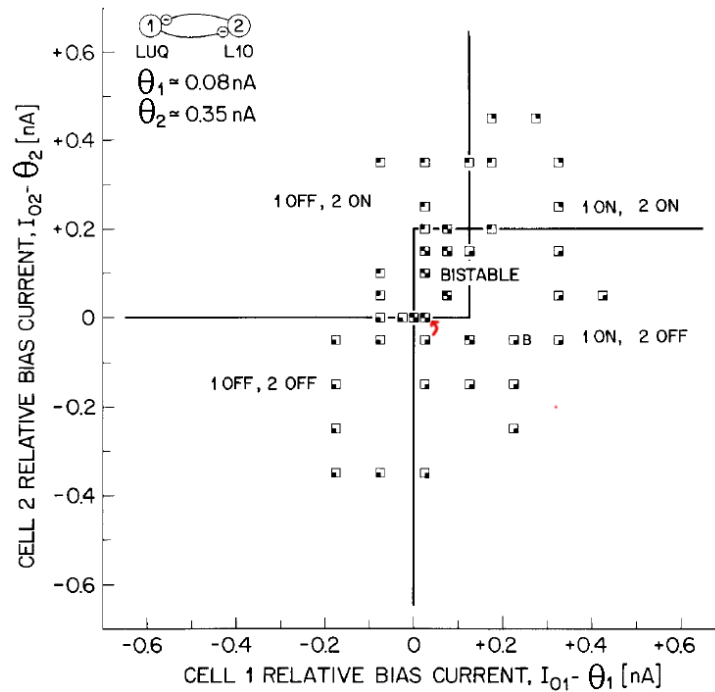Figure 31: Analysis of the stability diagram of a two-neuron circuit in vitro. From Kleinfeld, Raccuia-Behling and Chiel 1990.

1.7.4   Bistable circuits are a common motif

Bistable circuits show up in many places in vivo. They occur at a "low level" as part of oscillators that drive swimming in nudibranchs, such as Tritonia (Figure 32). Similar

19

circuits also drive whisking in the rodent (Figure 33). While the whisking circuit is comprised of many neurons, the cells cluster into one of two groups and, using the method of averaging that we will learn later in the course, can be reduced to a circuit of two "effective" neurons.

Figure 32: Escape swimming and the circuit and neuronal drive for escape swimming in Tritonia. Mixed sources including experiments of Willows and Getting.
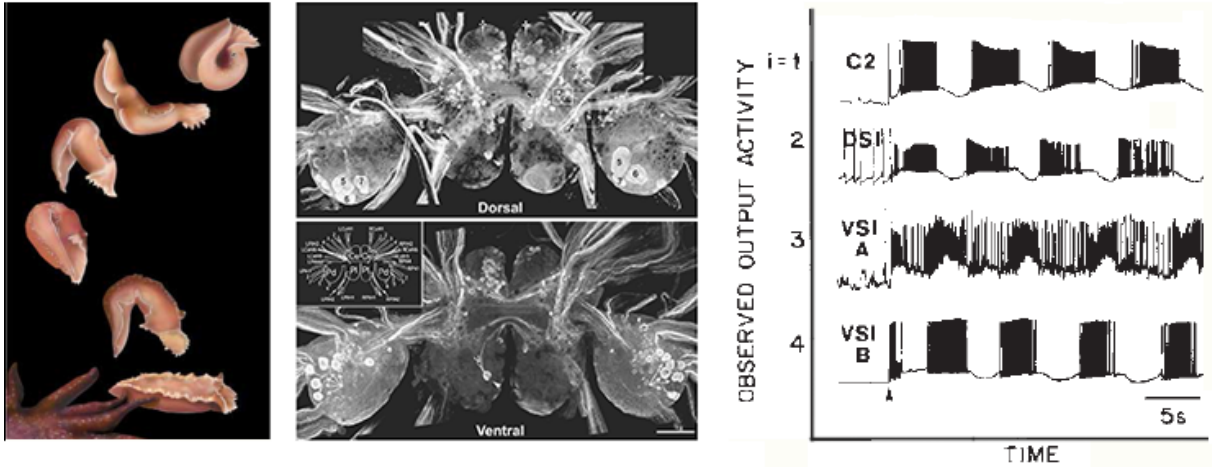
Figure 33: Whisking in the rodent is driven by both breathing, in a feedforward manner, and by an independent whisking oscillator. A detailed model of the oscillator with hundreds of neurons is reducible to one with reciprocal inhibition between two neurons for an autonomous whisking oscillator. Golomb, Moore, Fassihi, Takatoh, Prevosto, Wang and Kleinfeld, 2022.